Possibility of an electromechanical which-path interferometer

A. D. Armour*
The Blackett Laboratory, Imperial College of Science, Technology and Medicine, London SW7 2BZ, United Kingdom

M. P. Blencowe†
Department of Physics and Astronomy, Dartmouth College, Hanover, New Hampshire 03755

(Received 5 January 2001; revised manuscript received 28 March 2001; published 20 June 2001)

We investigate the possibility of an electromechanical which-path interferometer, in which electrons traveling through an Aharonov-Bohm ring incorporating a quantum dot in one of the arms are dephased by an interaction with the fundamental flexural mode of a radio-frequency cantilever. The cantilever is positioned so that its tip lies just above the dot and a bias is applied so that an electric field exists between the dot and the tip. This electric field is modified when an additional electron hops onto the dot, coupling the flexural mode of the cantilever and the microscopic electronic degrees of freedom. We analyze the transmission properties of this system and the dependence of interference fringe visibility on the cantilever-dot coupling and on the mechanical properties of the cantilever. The fringes are progressively destroyed as the interaction with the cantilever is turned up, in part due to dephasing arising from the entanglement of the electron and cantilever states and also due to the thermal smearing that results from fluctuations in the state of the cantilever. When the dwell time of the electron on the dot is comparable to or longer than the cantilever period, we find coherent features in the transmission amplitude. These features are washed out when the cantilever is decohered by its coupling to the environment.

DOI: 10.1103/PhysRevB.64.035311 PACS number(s): 85.35.Ds, 73.63.Kv, 73.23.Hk

I. INTRODUCTION

Which-path devices, such as the canonical two-slit interference experiment where a measurement is made of the path a particle takes, have a long history going back as far as the early debates about complementarity.[1,2] Recent interest in their investigation has been stimulated partly by advances in experimental techniques, which have lead to the realization of several different varieties of which-path systems in the laboratory,[3,4] and partly by accompanying developments in the theory of quantum measurement.[5–7] However, it is the realization that a which-path experiment provides a very convenient model system for developing and testing fundamental ideas about decoherence in mesoscopic systems[8,9] that has increased the level of interest within the solid-state physics community in particular.

Which-path experiments in solid-state systems were recently pioneered by Buks *et al.*[3] The solid-state analog of the two-slit interference experiment is the measurement of the oscillations in the current passing through an Aharonov-Bohm (AB) ring as a function of the applied magnetic field. The path taken by an electron may be probed by placing a measuring device close to one of the arms. Buks *et al.* incorporated a quantum dot in one of the arms in order to slow the electrons down, with a neighboring quantum point contact (QPC) serving as a which-path detector. An electron traveling around the arm of the ring containing the dot dwells on the dot for a finite amount of time before moving on. The presence of the dot alone does not destroy the coherence of the electron transport through the ring, so long as the dwell time of the electrons is sufficiently short,[10] but it does provide time for the electron to interact with an external measuring device. A QPC adjacent to the dot functions as a measuring device since it can be biased so that its conductance is very sensitive to changes in the occupancy of the dot: the passage of an electron via the path including the dot leaves behind which-path information in the QPC device, although actual knowledge of which path an electron took, so-called ''true which-path information,'' can only be obtained via further measurement.[11] In accord with theoretical predictions,[12–14] the experiment demonstrated that the interference fringes are degraded when the interaction between the electrons and the measuring device is sufficiently sensitive for information to be obtained that would help, even in principle, to determine which of the two possible paths an electron took.

The experiment of Buks *et al.* has close parallels with the well-known thought experiment (see, e.g., Secs. 1–6 of Ref. 2), in which a light source is used to detect through which slit an electron passes in a two-slit interference experiment. In both cases dephasing is effected by scatterers, each of which interacts once, and once only, with the interfering particle, and whose interactions with each other may safely be ignored. For the electron–light-scattering scheme,[2] the scatterers are photons that probe the electron's state directly, whereas in the solid-state experiment the scatterers are electrons in the QPC which interact with the electron on the dot via electrostatic coupling. However, because the electron has a finite dwell time on the dot, it has time to interact with more than one scatterer in the QPC, so that in this case dephasing can be achieved via a series of very weak interactions rather than a single strong event, as is the case in the photon thought experiment.

The present work is concerned with a variation on the system considered by Buks *et al.*, in which a radio-frequency mechanical cantilever is used, rather than a QPC, to determine which path an electron takes. A coupling between electrons residing on the dot (which is again on one of the AB

interferometer arms) and the cantilever, whose tip is suspended over the dot, can be set up by developing a uniform electric field between the tip of the cantilever and the base of the dot. Electrons on the dot couple approximately linearly to the cantilever position, thus leading to a coupling between the flexural phonon modes of the cantilever and the occupancy of the dot. Furthermore, because the coupling strength decays rapidly with increasing frequency and also the flexural mode spectrum of a cantilever is quite sparse, it turns out that for micron scale cantilevers only the fundamental flexural mode is relevant. Therefore, at low temperatures the cantilever can be treated as a single quantum-mechanical oscillator.

As a consequence of the cantilever having effectively only one degree of freedom, the electromechanical which-path interferometer exhibits qualitatively different behavior from the QPC which-path device. In particular, we find that the dephasing behavior of the electron due to the cantilever depends on the relative magnitudes of the electron dwell time on the dot and the cantilever period. When the dwell time is short compared to the cantilever period, the dephasing occurs in a way analogous to Einstein's recoiling slit thought experiment.[1,5] In contrast, when the dwell time of the electron on the dot is comparable to or longer than the period of the cantilever, a description of the dephasing in terms of the entanglement of the cantilever and electron states becomes more appropriate than a semiclassical picture of momentum transfer. The effectively harmonic nature of the cantilever motion means that the degree of entanglement between the cantilever and electronic states must be periodic, so long as the cantilever interacts only with the electron on the dot. If the dwell time of the electrons on the dot could be tuned to the cantilever period, then we would be able to erase all which-path information held in the state of the cantilever. This would give us direct evidence that the coupled cantilever and dot were behaving as a single coherent quantum system. However, in practice electron dwell times on a quantum dot have a distribution of values and so we can only obtain indirect evidence for the quantum coherence of the cantilever-dot system, such as the coherent exchange of energy quanta between the electron and the cantilever which give rise to side resonances in the elastic transmission amplitude of the device.

The environment of the cantilever influences its behavior in two important ways: over short time scales it destroys the cantilever's phase coherence, whilst over longer time scales it damps the cantilever's motion. The electromechanical which-path system we propose acts as a probe of the cantilever's decoherence due to it's interaction with the environment. We show that the cantilever's decoherence inhibits the coherent exchange of energy between the cantilever and the dot and hence manifests itself by washing out the side resonances in the elastic transmission amplitude.

The outline of this paper is as follows. In Sec. II we give our basic model for the electromechanical which-path device and show that the interference properties of the AB ring, modified to include the dot and cantilever, can be obtained by calculating the elastic transmission amplitude of the arm containing the dot. In Sec. III we describe a simple tight-binding model for an electron on a dot which is linearly coupled to the cantilever (treated as a quantum oscillator) and to propagating states in the leads. We show that recent work on inelastic resonant tunneling can be adapted to obtain the elastic transmission amplitude.

We present results for our model in Sec. IV, where we examine dephasing as a function of the dot-cantilever coupling in both the regime where the electron dwell time is short compared to the cantilever period and where they are comparable.

In Sec. V we examine the influence of the cantilever's environment on the dephasing produced by the cantilever when the dwell time is comparable to the period of the cantilever. We obtain a modified expression for the transmission through the arm with the dot when the cantilever is coupled to an environment which consists of a bath of oscillators.

In Sec. VI we outline the principal practical constraints on an electromechanical which-path device and discuss its feasibility using currently available technology. We draw our conclusions in Sec. VII and discuss ways in which the present work could be extended. Appendix A contains a detailed, classical analysis of the cantilever-dot coupling and the flexural mode spectrum of the cantilever which underpin the simplified model employed in the main text. Finally, Appendix B contains details of a general calculation of the effect of the cantilever environment on the transmission amplitude of the dot.

II. THEORETICAL MODEL

The ultimate goal of our analysis of the electromechanical which-path device is to obtain an expression for how the magnetoresistance of the AB ring varies as a function of the coupling between the cantilever and an electron on the dot. In particular, we want to determine how the amplitude and phase of the oscillation in the current through the device as the magnetic field is varied (i.e., the interference fringes) depend on the voltage between the cantilever and the dot. In order to simplify the analysis, we will consider only the case where the magnetoresistance is measured as an average over a time much longer than any other time scale in the problem.

Our model builds on the theoretical analysis of the QPC which-path experiment, carried out by a number of groups.[12–14] However, there are also close parallels between the system we consider and a quantum optical system analyzed recently,[15,16] in which radiation is used to drive an oscillator-mounted mirror into nonclassical states.

Since we are interested in the behavior of the system averaged over time, it is sufficient to work within the Landauer framework, so that our task of obtaining the average magnetoresistance is equivalent to calculating the transmission characteristics of the device.[17] The simplest way of thinking about the transmission probability through the AB ring is in terms of a two-slit experiment: the total transmission probability $\mathcal{T}$ is given by the coherent sum of amplitudes for transmission through the left and right arms, t_l and t_r,

$$\mathcal{T}=|t_l+t_r|^2. \tag{1}$$

This approach was employed by Yacoby *et al.*[10] in their analysis of experiments on AB rings with a quantum dot included in one arm. However, in that case this simple formalism proved inadequate as it neglects the contribution of electrons which have undergone multiple reflections. The contribution to the transmission of multiply reflected electrons leads to the enforcement of the Onsager-type relation for the conductance from source (S) to drain (D): $G_{DS}(B)=G_{DS}(-B)$, which must apply for a two-terminal device.[18–21] If the AB ring is modified to absorb electrons which are scattered backwards in the device, then the Onsager-type condition is no longer satisfied and the simple-minded formula (1) is valid. Buks *et al.* incorporated just such a modification in their AB ring and we shall limit our analysis to this case. We write $\tilde{t}_{\rm QD}$ for the transmission through the arm containing the dot and t_0 for the other amplitude. The presence of a magnetic flux Φ induces an additional relative phase shift between the two paths and so the transmission probability in the absence of the cantilever can be written as

$$\mathcal{T}=|t_0+\tilde{t}_{\rm QD}e^{i2\pi\Phi/\Phi_0}|^2=\mathcal{T}^{(0)}+2\,{\rm Re}[t_0^*\tilde{t}_{\rm QD}e^{i2\pi\Phi/\Phi_0}], \tag{2}$$

where Φ_0 is the flux quantum and $\mathcal{T}^{(0)}$ is the flux independent term of the transmission probability. In practice, the transmission through the arm with the dot is much less than that through the arm without the dot, $|\tilde{t}_{\rm QD}|\ll|t_0|$, and so $\mathcal{T}_0\approx|t_0|^2$.

When there is a nonzero interaction between the cantilever and the electron on the dot, we must explicitly include the fact that the transmission depends on the initial state of the cantilever. Since the cantilever contains a macroscopic number of atoms we assume that its initial state can always be described as a thermal mixture. Such a procedure will necessarily lead us to neglect short-time correlations between the cantilever states, but this will be unimportant if the magnetoresistance is averaged over a time which is long compared with the characteristic time scale for the thermalization of the cantilever's motion.[22] With the initial state of the cantilever assumed to be thermal, we have

$$\mathcal{T}=\sum_i\sum_f\rho_i[\langle i|t_0+\hat{t}_{\rm QD}e^{i2\pi\Phi/\Phi_0}|f\rangle \times(\langle i|t_0+\hat{t}_{\rm QD}e^{i2\pi\Phi/\Phi_0}|f\rangle)^*], \tag{3}$$

where $\hat{t}_{\rm QD}$ is an operator on cantilever states only, ρ_i is the usual thermal weight ($\rho_i=e^{-\beta\epsilon_i}/\Sigma_j e^{-\beta\epsilon_j}$, with $\beta=1/k_{\rm B}T$ and ϵ_i the energy of the state), and we have made no assumption about the final state of the cantilever mode. Because only the dot arm interacts with the cantilever the interference term is diagonal in the cantilever modes,

$$2\,{\rm Re}\left[\sum_i\rho_i t_0^*\langle i|\hat{t}_{\rm QD}|i\rangle e^{i2\pi\Phi/\Phi_0}\right]=2\,{\rm Re}[t_0^*\langle\tilde{t}_{\rm QD}\rangle e^{i2\pi\Phi/\Phi_0}], \tag{4}$$

where $\langle\tilde{t}_{\rm QD}\rangle$ is averaged over the cantilever thermal state. Thus, only elastic scattering processes contribute to the interference term.

At finite temperatures we also have to average the transmission amplitude for transport through the arm containing the dot over the Fermi distribution:[17]

$$\langle\tilde{t}_{\rm QD}\rangle=\int_0^\infty d\epsilon\left(-\frac{\partial f}{\partial\epsilon}\right)\langle t_{\rm QD}(\epsilon)\rangle. \tag{5}$$

The knowledge of the transmission amplitude allows us to obtain the amplitude of the periodic oscillations in the current, or in the language of a generic two-slit experiment, the visibility of the interference fringes. The visibility v in a two-slit experiment is defined in terms of the maximum and minimum signal (in this case current), measured at the peaks and valleys of the fringes, respectively,[23]

$$v=\frac{\max-\min}{\max+\min}. \tag{6}$$

In the case of the electromechanical which-path device considered here, the current is proportional to the transmission probability $\mathcal{T}$, given in Eq. (3). We can write the transmission amplitudes through the two arms in modulus-argument form, $\langle\tilde{t}_{\rm QD}\rangle=|\langle\tilde{t}_{\rm QD}\rangle|e^{i\alpha}$ and $t_0^*=|t_0|e^{-i\beta}$, so that the interference part of the transmission probability takes the form

$$2\,{\rm Re}[t_0^*\langle\tilde{t}_{\rm QD}\rangle e^{i2\pi\Phi/\Phi_0}] =2|t_0||\langle\tilde{t}_{\rm QD}\rangle|\cos(2\pi\Phi/\Phi_0+\alpha-\beta). \tag{7}$$

Hence in this case, the visibility of the fringes is

$$v=\frac{2|t_0||\langle\tilde{t}_{\rm QD}\rangle|}{\mathcal{T}^{(0)}}\simeq\frac{2|\langle\tilde{t}_{\rm QD}\rangle|}{|t_0|}. \tag{8}$$

The phase of the transmission amplitude determines the phase of the fringe pattern as a function of the magnetic field. Any change in the phase of the transmission amplitude should therefore be detectable as a change in the phase of the whole interference pattern.

In the absence of the dot, and for the ideal case of a ring in which both arms are identical, the transmission amplitudes for both arms are the same so that $\mathcal{T}_0=2|t_0|^2$ and the visibility is unity. This demonstrates the utility of v as a measure: it does not depend on the value of the total transmission probability through the device, but just on its interferometric properties.

In practice, a fringe visibility close to unity cannot be achieved. Apart from the obvious difficulty in constructing a ring in which both arms are identical, there are two further reasons why the ''intrinsic'' visibility is less than unity.[10] Firstly, there is more than one conduction channel in each arm and so the transport is never really a ''one-electron'' problem. Secondly, thermal smearing can play an important role, since the thermal smearing length is typically comparable to the size of the ring at temperatures of around 100

mK.[10] However, for our device the reduction in fringe visibility arising from sources other than the cantilever is irrelevant: all we require is that there should be a measurable change in the visibility of the fringes as the electric field coupling the dot and cantilever is turned on.

III. TRANSMISSION AMPLITUDE

In order to obtain the transmission amplitude for the arm of the AB ring containing the dot, we employ a standard tight-binding model for the dot and the leads to which it is coupled. In the Coulomb blockade regime, the quantum dot is modeled by a single localized state, at energy ϵ_0, which is coupled to sets of noninteracting, propagating states in the leads. The cantilever is treated as a single quantum oscillator mode of frequency ω_0, although the generalization to include a spectrum of modes is straightforward, as we discuss below. The total Hamiltonian of the interferometer arm can be written as the sum of two parts

$$\mathcal{H}=\mathcal{H}_0+\mathcal{H}_1, \tag{9}$$

with the noninteracting part

$$\mathcal{H}_0=\epsilon_0\hat{c}^\dagger\hat{c}+\sum_k\ (\epsilon_{kL}\hat{c}_{kL}^\dagger\hat{c}_{kL}+\epsilon_{kR}\hat{c}_{kR}^\dagger\hat{c}_{kR})+\hbar\omega_0\hat{a}^\dagger\hat{a}, \tag{10}$$

and the interacting part

$$\mathcal{H}_1=-\lambda\hat{c}^\dagger\hat{c}(\hat{a}+\hat{a}^\dagger)+\sum_k\ V_{kL}(\hat{c}_{kL}^\dagger\hat{c}+\hat{c}^\dagger\hat{c}_{kL})$$

$$+\sum_k\ V_{kR}(\hat{c}_{kR}^\dagger\hat{c}+\hat{c}^\dagger\hat{c}_{kR}), \tag{11}$$

where $\hat{c}$ and $\hat{a}$ operate on the states of the electron on the dot and the cantilever, respectively. The states in the left-hand (right-hand) leads have energies $\epsilon_{kL}(\epsilon_{kR})$ and are operated on by $\hat{c}_{kL}(\hat{c}_{kR})$, where the index k runs over propagating states in the leads. The matrix elements for hopping onto (off) the dot are given by V_{kL} (V_{kR}). The interaction between the electron on the dot and the cantilever is modeled as a linear coupling between the displacement of the flexural mode and the occupation of the dot, since when the electron is not on the dot there is no displacement of the cantilever.[24] We analyze the interaction between the cantilever and the dot in some detail in Appendix A, where the form of the interaction is derived in terms of the normal modes of the cantilever. We find that the coupling constant λ is given by the relation $\lambda=\xi eE\sqrt{\hbar/2m\omega_0}$ [see Eq. (A12)], where ξ is a geometrical factor of order one, E is the electric field experienced by the additional electron on the dot, m is the cantilever mass, and $e(>0)$ the electronic charge.

The energy-dependent amplitude $t_{\mathrm{QD}}(\epsilon)$ is calculated using the usual S-matrix formalism[25] employed in transport theory. The amplitude for transmission from a state of energy ϵ to one of energy ϵ' is given by the element of the S-matrix[25] linking propagating states in the left- and right-hand leads

$$\langle\epsilon',R|S|\epsilon,L\rangle=t_{\mathrm{QD}}(\epsilon,\epsilon'), \tag{12}$$

where $\langle\epsilon',R|(|\epsilon,L\rangle)$ is the state in the right- (left-) hand lead with energy $\epsilon'(\epsilon)$. The total transmission amplitude at energy ϵ is then obtained by integrating over the final-state energies

$$t_{\mathrm{QD}}(\epsilon)=\int_0^\infty t_{\mathrm{QD}}(\epsilon,\epsilon')d\epsilon'. \tag{13}$$

The S-matrix element for a single-electron tunneling from left to right through a single, localized, state which is coupled to a cantilever mode can be calculated using either the methods described by Wingreen *et al.*[25] or those of Glazman and Shekhter.[26] For initial and final states of the cantilever given by α_i and α_f, respectively, the relevant matrix element is

$$\langle\epsilon',\alpha_f,R|S|\epsilon,\alpha_i,L\rangle=-i\int\int\frac{dt_1dt_2}{\hbar^2}e^{-\eta(|t_1|+|t_2|)}$$

$$\times\langle\epsilon',\alpha_f,R|e^{i\mathcal{H}_0t_2/\hbar}\mathcal{H}_1\hat{G}_R(t_2-t_1)$$

$$\times\mathcal{H}_1e^{-i\mathcal{H}_0t_1/\hbar}|\epsilon,\alpha_i,L\rangle, \tag{14}$$

where $\hat{G}_R(t)=-i\Theta(t)e^{-i\mathcal{H}t/\hbar}$ and η is the usual small positive real number inserted to ensure convergence.

We want to calculate the visibility of the fringes and so we need only calculate the coherent part of the transmission probability, and hence the elastic transmission amplitude. To evaluate the elastic transmission amplitude we consider processes in which the state of the cantilever remains unchanged and so we write $\alpha_i=\alpha_f=\alpha$ and calculate an average over an ensemble of states of the cantilever (see the discussion in Sec. II above). Thus

$$\langle S\rangle=-V_R(\epsilon)V_L(\epsilon')\int\int\frac{dt_1dt_2}{\hbar^2}e^{-\eta(|t_1|+|t_2|)}$$

$$\times e^{i(\epsilon't_2-\epsilon t_1)/\hbar}\Theta(t_2-t_1)\langle0,\alpha|\hat{c}(t_2)\hat{c}^\dagger(t_1)|0,\alpha\rangle \tag{15}$$

with $|V_{L(R)}(\epsilon)|^2=\Sigma_k|V_{kL(R)}|^2\delta(\epsilon-\epsilon_{kL(kR)})$ and where $|0,\alpha\rangle$ is the state with no electrons on the localized level and the cantilever in state α.

We assume that the coupling to the leads is independent of energy over the range of interest and that it is symmetric so that we can write

$$\Gamma=\Gamma_{L(R)}=2\pi|V_{L(R)}|^2. \tag{16}$$

Since we are considering only the elastic part of the transmission amplitude the Green function will be invariant with respect to time. Hence, we change variables to $\tau=t_2-t_1$ and $t_0=t_1$, so that the Green function takes the form

$$G^R(\tau,t_0)=-i\Theta(\tau)\langle\hat{c}(\tau+t_0)\hat{c}^\dagger(t_0)\rangle \tag{17}$$

and the invariance with respect to translations in time is equivalent to the statement that the value of the Green func-

tion is independent of the choice of t_0. Averaging over t_0, and taking the limit $\eta \to 0^+$, the overall expression for the S-matrix element is then

$$\langle \epsilon', R|S|\epsilon, L\rangle = -i\frac{\Gamma}{2\pi}\int_0^\infty \frac{d\tau}{\hbar} e^{i\epsilon\tau/\hbar} G^R(\tau) \times 2\pi\delta(\epsilon-\epsilon'). \tag{18}$$

Thus, the final expression for the transmission amplitude of the dot is

$$\langle t_{\rm QD}(\epsilon)\rangle = -i\Gamma\int_0^\infty \frac{d\tau}{\hbar} e^{i\epsilon\tau/\hbar} G^R(\tau), \tag{19}$$

where the transmission amplitude is understood to be time-averaged in the sense described in Sec. II, and the relevant Green function is

$$G^R(\tau) = -i\Theta(\tau)\langle \hat{c}(\tau)\hat{c}^\dagger(0)\rangle, \tag{20}$$

where the expectation value is over a thermal distribution state of the cantilever with no electrons present. This result for the transmission amplitude is very similar to that studied by Aleiner *et al.*,[13] in their analysis of the QPC which-path device.

The Green function can be evaluated using either operator algebra techniques[26] or many-body perturbation theory,[25] and one obtains

$$G^R(\tau) = G_0^R(\tau) e^{-\phi(\tau)}, \tag{21}$$

where

$$G_0^R(\tau) = -i\Theta(\tau) e^{(-i\epsilon_0 - \Gamma/2)\tau/\hbar}, \tag{22}$$

and it has been assumed that the renormalization of the dot energy ϵ_0 due to coupling to the leads can be ignored. The factor due to coupling to the cantilever $\phi(\tau)$ can be obtained by calculating the contribution for the cantilever beginning and ending in a particular coherent state $|\nu\rangle$ and then carrying out a thermal average over all coherent states with appropriate weightings,

$$e^{-\phi(\tau)} = e^{i(\lambda/\hbar\omega_0)^2[\omega_0\tau - \sin(\omega_0\tau)]} e^{-(\lambda/\hbar\omega_0)^2[1-\cos(\omega_0\tau)]} \times \int \frac{d^2\nu}{\pi\bar{n}} e^{(\lambda/\hbar\omega_0)(\nu^*\mu - \nu\mu^*)} e^{-|\nu|^2/\bar{n}}, \tag{23}$$

where $\mu = e^{i\omega_0 t} - 1$. Evaluating the thermal average, we find

$$\phi(\tau) = \left(\frac{\lambda}{\hbar\omega_0}\right)^2 \{i[\sin(\omega_0\tau) - \omega_0\tau] + [1-\cos(\omega_0\tau)](1+2\bar{n})\}, \tag{24}$$

with $\bar{n}$ the thermal occupation of the cantilever mode.

It is clear that the thermal average leads to a much more rapidly decaying term, due to the extra factor of $2\bar{n}$. If the cantilever remained in a coherent state throughout then it would be far less effective, compared to the thermal state, at reducing the visibility of the fringes. This is because each coherent state affects the transmission amplitude in two different ways: the magnitude of the transmission is reduced by an amount which is independent of which state the cantilever is in and also a phase shift is induced whose size depends sensitively on the cantilever state. When we carry out the thermal average we are in effect averaging over a range of different phase shifts. Such a procedure effectively destroys the interference fringes whenever the thermal state includes contributions in which the phase differs by $\sim 2\pi$, irrespective of the magnitude of the transmission amplitude for each of the coherent states that constitute the thermal mixture. The thermal averaging time scale is given by the damping time of the cantilever which will typically be much larger than the dwell time of the electron on the dot. In this case, the loss of fringe visibility arising from thermal smearing is not due to which-path detection of individual electrons: a measurement of the current averaged over times shorter than the damping time but longer than the dwell time would resolve AB fringes with phase fluctuating in time. In contrast, the state-independent reduction in the transmission amplitude would give rise to a reduction in the fringe visibility even for the time-resolved measurement, signifying which-path detection. However, since we are working in a steady-state regime in which we consider measurements made over very long times we will not be able to make an explicit distinction between which-path detection and thermal smearing in this work.

We can repeat this calculation for the more general case of coupling to a whole series of noninteracting cantilever modes. The result has the same basic structure as before, but the cantilever factor $\phi(\tau)$ is modified and now takes the form of a sum of the contributions from each mode,[25,26]

$$\phi(\tau) = \sum_i \left(\frac{\lambda_i}{\hbar\omega_i}\right)^2 \{i[\sin(\omega_i\tau) - \omega_i\tau] + [1-\cos(\omega_i\tau)](1+2\bar{n}_i)\}, \tag{25}$$

where λ_i, ω_i, and $\bar{n}_i$ are the coupling constant, frequency, and thermal occupation number of the ith cantilever mode, respectively. However, we find that for the purposes of demonstrating the electromechanical which-path device we need only consider a single mode, as is discussed in Appendix A.

IV. RESULTS FOR AN ISOLATED CANTILEVER

The important question that we need to answer is the following: When does the cantilever destroy the AB fringes? There are two very different regimes which we can explore by varying the relative sizes of characteristic dwell time of the electron on the dot, $\tau_d = \hbar/\Gamma$, and the fundamental frequency of the cantilever.

(1) $\omega_0\tau_d \ll 1$: in this case the periodic behavior of the cantilever will not be relevant and the entanglement built up between the cantilever and electron states during the dwell time will be irreversible, leading to dephasing.

(2) $\omega_0\tau_d \sim 1$: in this regime the periodicity of the cantilever means that the entanglement of the cantilever and dot states caused by their interaction may be partially undone, or erased, although the distribution of electron dwell times will make the effect impossible to observe directly.

The first regime is easier to analyze theoretically, as the calculations can be done analytically and invite direct comparisons with the sliding-slit thought experiment. The case where the dwell time of the electron on the dot is comparable to the period of the cantilever has to be analyzed numerically. It is also complicated by the presence of the cantilever's environment which makes the entanglement of the cantilever and dot states irreversible by breaking the overall periodicity in the expression (19) for the transmission amplitude. In this section we calculate the magnitude and phase of the transmission amplitude in both regimes, neglecting the effect of the environment which we address in detail in Sec. V. This approach enables a clear picture to be built up of exactly how the environment affects the behavior of the cantilever-dot system.

A. Regime where $\omega_0 \tau_d \ll 1$

Since $\omega_0 \tau_d \ll 1$, we can simplify Eq. (19) for the transmission amplitude through the arm with the dot by expanding the harmonic functions to quadratic order in $\omega_0 \tau_d$. We obtain

$$\langle t_{\rm QD}(\epsilon)\rangle \simeq -\Gamma \int_0^\infty \frac{d\tau}{\hbar} e^{[i(\epsilon-\epsilon_0)-\Gamma/2]\tau/\hbar-(eE\Delta x_{\rm th}\tau)^2/2\hbar^2}, \tag{26}$$

where $\Delta x_{\rm th}=\sqrt{(2\bar{n}+1)(\hbar/2m\omega_0)}$ is the thermal position uncertainty of the cantilever and we have taken the geometrical factor in the coupling constant (A12) to be unity for simplicity. The integral on the right-hand side can now be evaluated to obtain

$$\langle t_{\rm QD}(\epsilon)\rangle \simeq -\sqrt{\frac{\pi}{2}}\left(\frac{\Gamma}{eE\Delta x_{\rm th}}\right)\exp\left(\frac{[\Gamma/2-i(\epsilon-\epsilon_0)]^2}{2(eE\Delta x_{\rm th})^2}\right) \times \mathrm{Erfc}\left(\frac{\Gamma/2-i(\epsilon-\epsilon_0)}{\sqrt{2}eE\Delta x_{\rm th}}\right). \tag{27}$$

If we ignore, for the moment, the thermal width of the electron-energy distribution in the leads, then we can deduce from this expression a rough criterion for dephasing in the region close to the electronic resonance:

$$eE\Delta x_{\rm th} > \Gamma, \tag{28}$$

or written in another way,

$$eE\tau_d > \frac{\hbar}{\Delta x_{\rm th}}. \tag{29}$$

Practical considerations (see Sec. VI) restrict the dwell time to be a few ns or less and place an upper bound on the electric field: $E \sim 10^5$ V/m. Thus, the destruction of the interference fringes requires $\Delta x_{\rm th} > 10^{-2}$ Å, a value which is certainly achievable.

As previously discussed, the loss of fringe visibility is not only associated with which-path detection, but with thermal smearing as well. We can obtain the condition for which-path detection by setting the cantilever temperature to zero in Eq. (29):

$$eE\tau_d > \frac{\hbar}{\Delta x_{\rm zp}} = 2\Delta p_{\rm zp}, \tag{30}$$

where $\Delta x_{\rm zp}=\sqrt{\hbar/2m\omega_0}$ denotes the zero-point position uncertainty. Because the reduction in the transmission amplitude due to each different coherent state is the same [cf., Eq. (23)], this condition holds independently of which coherent state the cantilever is in. Thus, we find that for which-path detection to occur the classical impulse delivered to the cantilever during the dwell time must exceed twice the zero-point momentum uncertainty of the cantilever.

Our result is equivalent to that obtained by Bohr in his famous discussion of Einstein's sliding-slit *gedanken* experiment.[1] In that case Bohr argued that in order to detect the passage of an electron through a given slit, the momentum uncertainty in the slit must be less than the impulse transferred by the passing electron, thus necessitating a corresponding latitude in position of the slits (via the uncertainty principle) which in turn washes out the fringes by causing large phase shifts (i.e., $\sim 2\pi$) for successive electrons. However, these phase shifts are not associated with any kind of thermal fluctuation; instead, they arise from the position uncertainty of the quantum state of the slits.

At finite temperatures we must take into account not only the thermal state of the cantilever, but also the fact that the electron energies are spread over a range $\sim 4k_{\rm B}T$ around the Fermi energy. We must therefore average the transmission amplitude over energy, weighted by the derivative of the Fermi distribution function [see Eq. (5)],

$$\langle \tilde{t}_{\rm QD}\rangle = \int_0^\infty d\epsilon \frac{\langle t_{\rm QD}(\epsilon)\rangle}{4k_{\rm B}T}\mathrm{sech}^2\left(\frac{\epsilon-\epsilon_0}{2k_{\rm B}T}\right), \tag{31}$$

where we have assumed that the bias across the device is small enough for a linear-response approach to be valid and that the average Fermi energy in the leads is tuned to the resonance ϵ_0. The effect of this procedure is to reduce both the coherent transmission amplitude itself and the influence the cantilever has on it. The explanation for this unexpected feature can be found by comparing the transmission amplitude $\langle t_{\rm QD}(\epsilon)\rangle$ at and away from the resonance. Whilst the transmission amplitude at, or close to, resonance decays rapidly with increasing coupling to the cantilever, the situation is reversed when the electron energy is far from resonance, where the transmission amplitude is *enhanced* by the interaction with the cantilever. The reduction in dephasing efficiency due to the thermal averaging over the electron-energy distribution makes an interesting contrast to the effect of the thermal average over cantilever states, which increases the dephasing rate substantially.

Figure 1 illustrates the effect of increasing the dimensionless coupling constant $\kappa=\lambda/\hbar\omega_0$ on the magnitude of the resonant transmission amplitude $|\langle t_{\rm QD}(\epsilon_0)\rangle|$, with and without averaging over the thermal width of the electron-energy distribution in the leads. For this example, we have taken

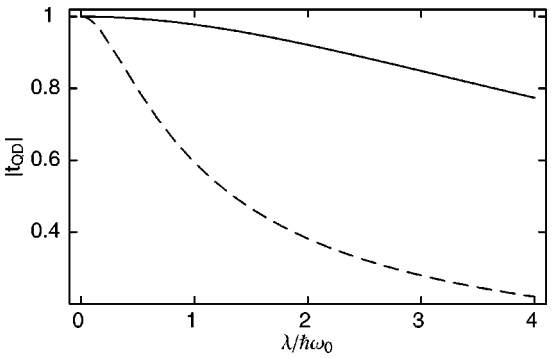

FIG. 1. Magnitude of the transmission amplitude $|\langle t_{QD}\rangle|$ at resonance for a cantilever with $\Gamma/\hbar\omega_0=10$ as a function of the dimensionless coupling constant $\kappa=\lambda/\hbar\omega_0$. The dashed curve is obtained without an average over incident electron energies, while the full curve includes the averaging. The amplitudes are normalized to one at $\kappa=0$.

$\omega_0=140$ MHz and $T=20$ mK (giving a thermal occupation $\bar{n}=18$), $m=8\times10^{-20}$ kg, and assumed κ to have a maximum value of about 3, consistent with the analysis of the cantilever-dot coupling in Appendix A. The effect of the thermal broadening of electron energies in reducing the efficiency of the cantilever to cause dephasing is clear.

It is important to note that our treatment is entirely restricted to a one-electron picture of transport. Such an approach is valid so long as the electron gas in the leads and the dot itself is nondegenerate. When the electron temperature drops towards zero the interactions between electrons can no longer be ignored and so our model and the results which follow from it become inapplicable. At $T=0$ and in the weak-bias limit, inelastic transport through the dot would become impossible: with the absence of unoccupied states below the Fermi level and the cantilever in the ground state an electron is unable to exchange energy quanta with the cantilever.

B. Regime where $\omega_0\tau_d\sim1$

In the regime where the dwell time of the electron on the dot approaches the period of the cantilever, the system takes on a rather different character, as the dephasing interaction between the cantilever and the electron on the dot is no longer a brief scattering event, but a sustained interaction. In this regime we would expect to see evidence of the periodic behavior of the cantilever, such as side resonances in the elastic transmission amplitude, but in practice these would have to compete with thermal effects that tend to wash out fine structure in the transmission characteristics.

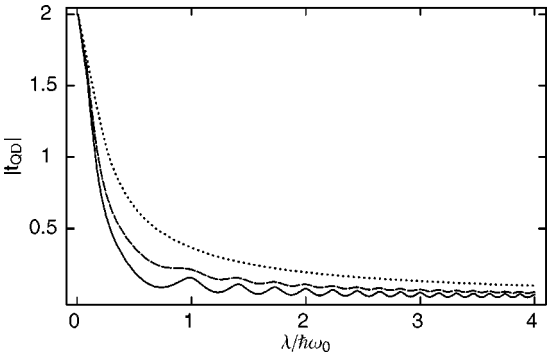

FIG. 2. Magnitude of the resonant transmission amplitude $|\langle t_{QD}\rangle|$ as a function of coupling constant κ for $\Gamma/\hbar\omega_0=2$ (dotted curve), 1 (dashed curve), and 0.5 (full curve).

In order to calculate the transmission amplitude, it is convenient to recast our earlier expression (19) in the form

$$\langle t_{QD}(\epsilon)\rangle=-\frac{\Gamma}{\hbar\omega_0}\frac{e^{-(\lambda/\hbar\omega_0)^2(2\bar{n}+1)}}{1-e^{-(2\pi/\omega_0)(\{i[\epsilon_0-(\lambda^2/\hbar\omega_0)-\epsilon]/\hbar\}+\Gamma/2\hbar)}}\times\int_0^{2\pi}d\tau'\exp\left\{\frac{-\tau'}{\omega_0}\left[\frac{i}{\hbar}\left(\epsilon_0-\frac{\lambda^2}{\hbar\omega_0}-\epsilon\right)+\frac{\Gamma}{2\hbar}\right]-i\left(\frac{\lambda}{\hbar\omega_0}\right)^2\sin(\tau')+(2\bar{n}+1)\left(\frac{\lambda}{\hbar\omega_0}\right)^2\cos(\tau')\right\},\tag{32}$$

where $\tau'=\omega_0\tau$. Of course, to model a practical experiment, we also need to average over the energy ϵ to take into account the effect of electron temperature. However, we look first at the dependence of the transmission amplitude on the incident energy. Although this would require ''monochromatic'' electrons, important insight is gained into the behavior of the system which in practice may be obscured by thermal effects.

In Fig. 2 the magnitude of the resonant transmission amplitude is plotted against the coupling κ for $\Gamma/\hbar\omega_0=2$, 1, and 0.5, and with $\bar{n}=18$. The behavior is similar in all three cases for small κ, with a rapid decay in the magnitude of the transmission amplitude, due to dephasing caused by a combination of which-path detection and thermal fluctuations in the state of the cantilever. Notice, however, that for $\Gamma/\hbar\omega_0=1$, oscillations eventually develop in the transmission, and that these become even more pronounced for $\Gamma/\hbar\omega_0=0.5$.

In order to clarify the origin of the oscillations in $|\langle t_{QD}(\epsilon)\rangle|$, Fig. 3 plots the evolution of the amplitude and phase of the transmission amplitude as functions of both the coupling constant κ and the detuning energy $\epsilon-\epsilon_0$ for $\Gamma/\hbar\omega_0=0.5$ and $\bar{n}=18$. It is now clear that there are side resonances at $\epsilon-\epsilon_0+\lambda^2/\hbar\omega_0=\pm\hbar\omega_0,\pm2\hbar\omega_0,\ldots,$ and that these resonances drift in energy as the value of κ is increased.[25,27] It is this drift which is responsible for the oscillations in $|\langle t_{QD}(\epsilon)\rangle|$ as a function of the coupling κ for given fixed ϵ.

Note that if the cantilever temperature is set equal to zero, i.e., it is in its ground state, $\bar{n}=0$, then side resonances are still observed, but only on one side of the main peak, at $\epsilon-\epsilon_0+\lambda^2/\hbar\omega_0=+\hbar\omega_0,+2\hbar\omega_0,\ldots$. This is because in its ground state the cantilever can only absorb energy quanta.

Under the conditions $k_BT\gg\hbar\omega_0$, $\kappa\sim1$, and near resonance, Eq. (32) has the following asymptotic approximation:

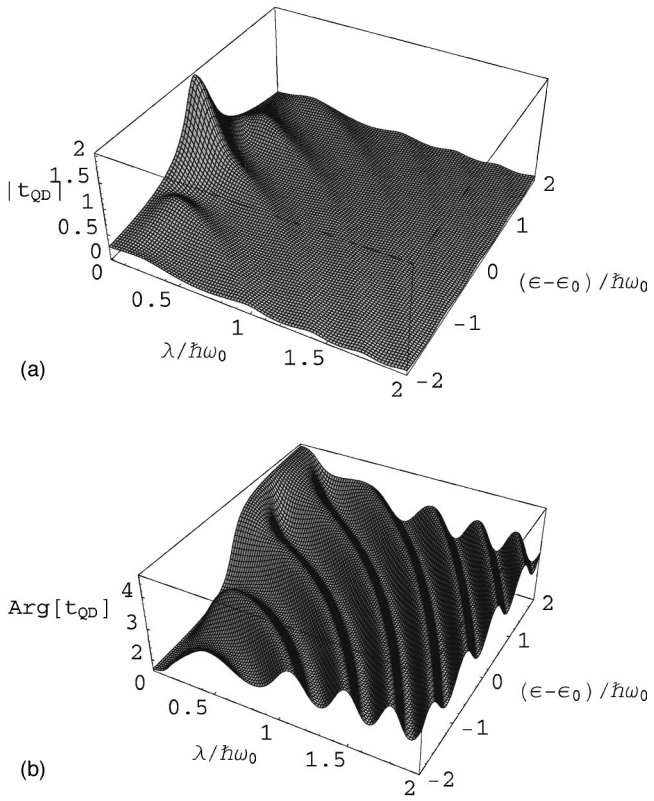

FIG. 3. (a) Magnitude of the transmission amplitude $|\langle t_{\mathrm{QD}}\rangle|$ and (b) the phase for a cantilever with $\Gamma/\hbar\omega_0=0.5$ as a function of coupling constant κ and the energy detuning $\epsilon-\epsilon_0$. The average over the electron-energy distribution has not been performed.

$$\langle t_{\mathrm{QD}}(\epsilon)\rangle \sim -\frac{\Gamma}{2\lambda}\sqrt{\frac{\pi\hbar\omega_0}{k_{\mathrm{B}}T}} \times\left\{\frac{1+e^{-(2\pi/\hbar\omega_0)[i(\epsilon_0-\lambda^2/\hbar\omega_0-\epsilon)+\Gamma/2\hbar]}}{1-e^{-(2\pi/\hbar\omega_0)[i(\epsilon_0-\lambda^2/\hbar\omega_0-\epsilon)+\Gamma/2\hbar]}}\right\}. \tag{33}$$

The various above-discussed features in the transmission amplitude dependence on coupling and energy can be clearly seen in this simplifying approximation.

Side resonances are a familiar feature in tunneling problems, but unlike those found here they are usually associated with inelastic processes. However, as was first shown by Jauho and Wingreen,[27] who considered the classical-oscillator version of the problem that we address, such resonances can also occur in the elastic transmission amplitude. Side resonances in the elastic transmission indicate coherent or virtual exchange of energy quanta between the electron on the dot and the cantilever, with no net energy interchange over the dwell time of the electron. In a fully quantum-mechanical system, these processes must rely on the coupled cantilever-electron system maintaining its phase coherency and so we may expect that the influence on the cantilever of its environment should be detectable, at least in principle, via its effect on these resonances.

The side resonances have a separation in energy of $\hbar\omega_0$, but for any practically realizable system the thermal energy scale will be much larger, as we discuss in detail in Sec. VI. However, in the regime where $\hbar\omega_0 \ll k_{\mathrm{B}}T$, averaging over the thermal distribution of electron energies will wash out the side resonances. This means that it would not be possible to find any trace of the coherent exchange of energy quanta between the cantilever and the electron on the dot in the transmission characteristics. Only if the electron-energy width could be lowered or the frequency raised to the point where $\hbar\omega_0 \sim k_{\mathrm{B}}T$ would we then expect such features to be visible. Note, in the case of photon-assisted tunneling the photon energy can be made comparable with $k_{\mathrm{B}}T$ without difficulty.[27]

V. INFLUENCE OF ENVIRONMENT ON CANTILEVER

Thus far, we have treated the cantilever-dot system as isolated, thereby ignoring the effect of the environment on their degrees of freedom. This approximation is valid when the dwell time of the electron on the dot is short compared to the decoherence time of the cantilever, as will most certainly be the case for $\omega_0\tau_d \ll 1$. However, there is no reason to assume that this will also be the case when $\omega_0\tau_d \sim 1$. Indeed, we would like to know how the environment of the cantilever affects the coherent oscillations which occur in the transmission amplitude as a function of the coupling strength (for monochromatic electrons). Intuitively, we expect that the decoherence arising from the cantilever's environment should wash out the side resonances in the transmission amplitude, but a detailed calculation is required to determine the cantilever quality (Q) factor range for this to occur.

In general, both the interaction between the dot electron and its local environment (other electrons, phonons, photons, etc. in the dot region) and the interaction between the cantilever and its environment (the other collective vibrational modes, as well as internal electronic degrees of freedom, external photons, gas molecules, etc.) will contribute to the decoherence. However, since we can always measure the properties of the fringes with the dot-cantilever interaction turned off for an arbitrary dwell time ($\tau_d=\hbar/\Gamma$), we need only consider the additional effect of the cantilever's environment, as the electron's environment can be included via a renormalization of the zero-electric-field transmission amplitude.

A. Estimate of cantilever decoherence time

We can obtain a rough estimate of the time scale over which superpositions of cantilever states, resulting from the coupling to the dot electron, are likely to be decohered by the environment by using a simple, heuristic approach which models the environment as an infinite set of harmonic oscillators.[28,16] This approach leads to the prediction that for a system with a classical damping rate γ_c, a linear superposition of two different coherent states whose centers are a distance Δx apart, where Δx is greater than the thermal de Broglie wavelength, $\lambda_{\mathrm{th}}=\hbar/\sqrt{2mk_{\mathrm{B}}T}$, will decohere at a rate γ_d, given by

$$\gamma_d \sim \frac{2m\gamma_c k_{\mathrm{B}}T(\Delta x)^2}{\hbar^2}. \tag{34}$$

However, we cannot apply this heuristic rule directly to the coupled cantilever-dot system as the displacement of the cantilever is a continuously varying function. An estimate for the decoherence rate of the cantilever can only be obtained using this method if the further approximation of averaging over the cantilever displacement is made.[16] If the cantilever starts in any given coherent state when the electron arrives on the dot, then the state of the cantilever at time t later will be a different coherent state centered a distance Δx apart from the point on which the initial state was centered, where

$$\Delta x(t) = \sqrt{\frac{2\hbar}{m\omega_0}}\kappa[1-\cos(\omega_0 t)]. \tag{35}$$

Thus we can obtain an estimate for the decoherence rate γ_d of the cantilever due to its environment for the case where $\tau_d\omega_0 = 1$ by averaging this displacement over the cantilever period[16]

$$\gamma_d \sim \frac{1}{(2\pi/\omega_0)}\frac{4\kappa^2\gamma_c k_B T}{\hbar\omega_0}\int_0^{2\pi/\omega_0} dt[1-\cos(\omega_0 t)]^2$$

$$= 6\kappa^2\gamma_c\frac{k_B T}{\hbar\omega_0}. \tag{36}$$

For a nanotube cantilever of frequency ~ 140 MHz (see Appendix A), the Q factor[29] can be of order 500 and so the classical damping rate γ_c will be of order 3×10^5 s^{-1}. Thus, at a temperature of 20 mK, our heuristic expression for the decoherence rate of the nanotube cantilever gives $1/\gamma_d \sim 3\times 10^{-9}$ s for $\kappa \simeq 3$. This result signals that the decoherence of the cantilever due to its environment has an effect whenever the dwell time approaches a magnitude of order 1 ns.

Whilst the heuristic model we have outlined is very useful for estimating whether or not the cantilever's environment is relevant for the calculation of the transmission amplitude, it is not expected to be very accurate, as it is an approximation even of the rule-of-thumb given by Eq. (34). In order to improve on this estimate, we must enlarge our simple model by adding to the system Hamiltonian (9) the cantilever's environment, modeled as an infinite bath of harmonic oscillators with linear coupling to the cantilever. Modeling the environment in this way is of course itself a fairly serious approximation. However, this approximation is ubiquitous in one form or another throughout the theory of open quantum systems.[30,28,31,32] By extending our calculation to include this model of the cantilever's environment, we can obtain predictions for how the transmission properties of our which-path device depend on the decoherence rate of the cantilever. Thus, we can use our theory to predict how changing the Q factor of the cantilever affects the interference fringes.

B. Transport properties with environmental coupling

The standard model of the environment that we use is an infinite bath of harmonic oscillators that interact linearly with the cantilever, but do not interact with each other. We have to assume an infinite bath of oscillators in order to have a reservoir which remains in thermal equilibrium despite contact with the cantilever. The infinite oscillator-bath model of the environment is also equivalent to a quantum Langevin formalism in which the cantilever operators have an equation of motion containing a damping term and a thermal noise operator arising from the reservoir.

We begin by considering just the interaction between the cantilever and its environment, before going on to include the effect of an electron on the dot and hence obtaining the transmission amplitude including the environment. The cantilever-environment Hamiltonian can be written as[33,34]

$$\mathcal{H}^c = \hbar\omega_0\hat{a}^\dagger\hat{a} + \sum_\omega \hbar\omega\hat{A}^\dagger(\omega)\hat{A}(\omega) + \sum_\omega [g(\omega)\hat{a}^\dagger\hat{A}(\omega) + g^*(\omega)\hat{A}^\dagger(\omega)\hat{a}], \tag{37}$$

where the cantilever states are again operated on by $\hat{a}$, the bath oscillator of frequency ω is operated on by $\hat{A}(\omega)$, and the coupling constants $g(\omega)$ depend on the bath oscillator frequency.

Using the Hamiltonian $\mathcal{H}^c$, the equation of motion for $\hat{a}$ in the interaction picture is readily obtained,[33]

$$\dot{\hat{a}}(t) = (-i\omega-\gamma)\hat{a}(t) - \hat{F}(t), \tag{38}$$

where

$$\hat{F}(t) = i\sum_\omega g(\omega)\hat{A}(\omega,0)e^{-i\omega t} \tag{39}$$

and the damping coefficient γ is given by

$$\gamma = \pi\eta_b(\omega_0)|g(\omega_0)|^2, \tag{40}$$

where $\eta_b(\omega)\delta\omega$ is the number of bath oscillators in the spectral range $\delta\omega$. The coefficient γ provides the bridge between the model and experiment, as it is simply related to the rate at which the system loses energy after being excited (i.e., the classical damping rate),[34] $\gamma_c = 2\gamma$.

Integration of the equation of motion for $\hat{a}(t)$, and a similar one for $\hat{a}^\dagger(t)$, leads to explicit expressions for $\hat{a}(t)$ and $\hat{a}^\dagger(t)$,

$$\hat{a}(t) = \hat{a}(0)e^{(-i\omega_0-\gamma)t} - e^{(-i\omega_0-\gamma)t}\int_0^t dt'\hat{F}(t')e^{(i\omega_0+\gamma)t'}, \tag{41}$$

$$\hat{a}^\dagger(t) = \hat{a}^\dagger(0)e^{(i\omega_0-\gamma)t} - e^{(i\omega_0-\gamma)t}\int_0^t dt'\hat{F}^\dagger(t')e^{(-i\omega_0+\gamma)t'}. \tag{42}$$

The time $t=0$ holds a special place in the theory since it is the time at which the interactions between the cantilever and the bath are turned on and so the cantilever and the bath are apparently quite independent at this instant. However, this need not be the case and certainly would not be appropriate for the system we are considering. In order to specify the model completely we need to give the expectation values at $t=0$ for both the cantilever and the bath. If we set the initial expectation values of the cantilever to be those of a thermal state at the same temperature as the bath, then we

can describe the case in which the cantilever has been interacting with the bath for a time much longer than the damping time, $1/\gamma_c$, *before* $t=0$ and so is in equilibrium with the bath. Our only assumption is that quantum correlations between the cantilever and the bath can be neglected at $t=0$, the usual assumption made in calculating decoherence rates.

The expectation values are over products of cantilever and environment states. We eventually want to calculate the transmission amplitude for an electron interacting with a cantilever which is initially in a thermal state and so we choose to define the $t=0$ expectation values as

$$\langle \cdots \rangle = \frac{\mathrm{Tr}[\cdots e^{-\mathcal{H}_0^c/k_B T}]}{\mathrm{Tr}[e^{-\mathcal{H}_0^c/k_B T}]}, \tag{43}$$

where the Hamiltonian without interactions is

$$\mathcal{H}_0^c = \hbar\omega_0 \hat{a}^\dagger \hat{a} + \sum_\omega \hbar\omega \hat{A}^\dagger(\omega)\hat{A}(\omega), \tag{44}$$

and T defines the fixed temperature of the environment. Using this definition we find

$$\begin{aligned} \langle \hat{A}(\omega,0)\rangle &= 0, \\ \langle \hat{A}(\omega,0)\hat{A}(\omega',0)\rangle &= 0, \\ \langle \hat{A}^\dagger(\omega,0)\hat{A}(\omega',0)\rangle &= \delta_{\omega\omega'} N(\omega), \end{aligned} \tag{45}$$

with

$$N(\omega) = \frac{1}{e^{\hbar\omega/k_B T}-1}. \tag{46}$$

For the cantilever itself the values of the zero-time correlation functions represent the initial conditions of the problem. In thermal equilibrium with the environment at temperature T,

$$\begin{aligned} \langle \hat{a}(0)\rangle &= 0, \\ \langle \hat{a}(0)\hat{a}(0)\rangle &= 0, \\ \langle \hat{a}^\dagger(0)\hat{a}(0)\rangle &= \overline{n}, \end{aligned} \tag{47}$$

with

$$\overline{n} \equiv N(\omega_0) = \frac{1}{e^{\hbar\omega_0/k_B T}-1}. \tag{48}$$

The purpose of extending the analysis to include the interactions between the cantilever and its environment is to see how they modify the interaction between the cantilever and the electron *whilst it is on the dot*. Therefore we can choose our origin of time, and hence the definition of the initial cantilever state, to be the time when the electron jumps onto the dot. There is no need to explicitly include the interaction with the bath before the electron hops onto the dot as it is already implicitly included by assuming the cantilever is in a thermal state at temperature T. However, when the electron is on the dot it drives the cantilever away from equilibrium and we now need to include the interaction with the environment explicitly to model the behavior of the cantilever-dot system as accurately as possible.

We obtain the transmission amplitude for the dot, including the effect of the cantilever's environment by applying the S matrix we used in Sec. III to a generalization of the Hamiltonian (9) which includes the coupling of the cantilever to the bath of oscillators,

$$\mathcal{H} = \epsilon_0 \hat{c}^\dagger \hat{c} + \mathcal{H}^c + \mathcal{H}_1 + \sum_k \left(\epsilon_{kL}\hat{c}_{kL}^\dagger \hat{c}_{kL} + \epsilon_{kR}\hat{c}_{kR}^\dagger \hat{c}_{kR}\right), \tag{49}$$

where $\mathcal{H}_1$, given by Eq. (11), describes the electron-cantilever coupling and the cantilever-environment part $\mathcal{H}^c$ is given by Eq. (37).

Using the methods of Glazman and Shekhter,[26] we can again separate out the electronic part of the transmission amplitude from the average over cantilever states, and so we find

$$\langle t_{\mathrm{QD}}(\epsilon)\rangle = -\Gamma \int_0^\infty \frac{dt}{\hbar} e^{[i(\epsilon-\epsilon_0)-\Gamma/2]t/\hbar} \left\langle \mathrm{T}_t e^{-i\int_0^t W_I(t')dt'/\hbar}\right\rangle. \tag{50}$$

The term in angled brackets on the right-hand side is known as the influence functional, T_t is the time-ordering operator, and $W_I(t)$ is the electron-cantilever coupling defined in the interaction picture

$$W_I(t) = -e^{i\mathcal{H}^c t/\hbar}\lambda(\hat{a}^\dagger + \hat{a})e^{-i\mathcal{H}^c t/\hbar} = -\lambda[\hat{a}^\dagger(t) + \hat{a}(t)], \tag{51}$$

where $\hat{a}(t)$ and $\hat{a}^\dagger(t)$ are given by Eqs. (41) and (42) above.

Here, we shall carry out a much simpler, approximate calculation of the influence functional which involves performing a second-order expansion in λ and then reexponentiating. In Appendix B it is shown that this approximate calculation in fact coincides with the exact result obtained from a full calculation.

The expansion to second order gives

$$\left\langle \mathrm{T}_t e^{-i\int_0^t W_I(t')dt'/\hbar}\right\rangle = 1 - i\int_0^t \frac{dt'}{\hbar}\langle W(t')\rangle + (-i)^2 \times \int_0^t \frac{dt'}{\hbar}\int_0^{t'} \frac{dt''}{\hbar}\langle W(t')W(t'')\rangle. \tag{52}$$

The next step is to evaluate the correlation functions which arise in the first- and second-order terms in the expansion of the influence functional. At first order

$$\langle W(t')\rangle = -\lambda\langle[\hat{a}(t') + \hat{a}^\dagger(t')]\rangle, \tag{53}$$

and at second order

$$\langle W(t')W(t'')\rangle = \lambda^2\{\langle \hat{a}(t')\hat{a}(t'')\rangle + \langle \hat{a}(t')\hat{a}^\dagger(t'')\rangle + \langle \hat{a}^\dagger(t')\hat{a}(t'')\rangle + \langle \hat{a}^\dagger(t')\hat{a}^\dagger(t'')\rangle\}, \tag{54}$$

where $t' \geqslant t''$.

We can calculate all the correlation functions using the initial conditions defined above and the standard results of quantum Langevin theory.[33,34] We start by observing that three of the five correlation functions are zero,

$$\langle \hat{a}(t')\hat{a}(t'')\rangle = \langle \hat{a}^\dagger(t')\hat{a}^\dagger(t'')\rangle = 0 \tag{55}$$

and

$$\langle [\hat{a}(t') + \hat{a}^\dagger(t')]\rangle = 0. \tag{56}$$

These results follow from the definitions above, since correlators of the type $\langle \hat{a}(0)\hat{F}(t)\rangle$ decouple into products of one-time correlation functions and the definitions imply that $\langle \hat{F}(t)\rangle = \langle \hat{F}(t')\hat{F}(t'')\rangle = 0$. For the other two correlation functions, we have

$$\langle \hat{a}(t')\hat{a}^\dagger(t'')\rangle = (\bar{n}+1)e^{-i\omega_0(t'-t'')}e^{-\gamma(t'-t'')}, \tag{57}$$

$$\langle \hat{a}^\dagger(t')\hat{a}(t'')\rangle = \bar{n}e^{i\omega_0(t'-t'')}e^{-\gamma(t'-t'')}. \tag{58}$$

Thus, we again find

$$\langle t_{\mathrm{QD}}(\epsilon)\rangle = -\Gamma\int_0^\infty \frac{dt}{\hbar} e^{[i(\epsilon-\epsilon_0)-\Gamma/2]t/\hbar} e^{-\phi(t)}, \tag{59}$$

but now with

$$\phi(t) = \frac{\lambda^2}{\hbar^2}\int_0^t dt' \int_0^{t'} dt'' e^{-\gamma(t'-t'')} \times [(\bar{n}+1)e^{-i\omega_0(t'-t'')} + \bar{n}e^{i\omega_0(t'-t'')}], \tag{60}$$

where we have reexponentiated the expansion in λ.

Carrying out a change of variables to $\tau = t' - t''$, the integrals are readily evaluated to give

$$\phi(t) = \left(\frac{\lambda}{\hbar}\right)^2\left[\frac{(\bar{n}+1)}{(\gamma+i\omega_0)}\left(t + \frac{e^{-(\gamma+i\omega_0)t}-1}{\gamma+i\omega_0}\right) + \frac{\bar{n}}{(\gamma-i\omega_0)}\left(t + \frac{e^{-(\gamma-i\omega_0)t}-1}{\gamma-i\omega_0}\right)\right]. \tag{61}$$

Setting $\gamma = 0$, one may verify that Eq. (61) indeed reduces to expression (24) in the absence of the environment.

Under the conditions $Q \gg 1$, $k_B T \gg \hbar\omega_0$, $\kappa \sim 1$, and near resonance, the transmission amplitude (59) has the following asymptotic approximation:

$$\langle t_{\mathrm{QD}}(\epsilon)\rangle \sim -\frac{\Gamma}{2\lambda}\sqrt{\frac{\pi\hbar\omega_0}{k_B T}}\left\{\frac{1+e^{-(2\pi/\hbar\omega_0)[i(\epsilon_0-\lambda^2/\hbar\omega_0-\epsilon)+\Gamma/2\hbar+(\kappa^2\gamma_c k_B T/\hbar\omega_0)]}}{1-e^{-(2\pi/\hbar\omega_0)[i(\epsilon_0-\lambda^2/\hbar\omega_0-\epsilon)+\Gamma/2\hbar+(\kappa^2\gamma_c k_B T/\hbar\omega_0)]}}\right\}. \tag{62}$$

Note that this approximation differs from the earlier-derived one for the transmission amplitude in the absence of the environment, Eq. (33), merely by the replacement of $\Gamma/2\hbar$ with $\Gamma/2\hbar + (\kappa^2\gamma_c k_B T/\hbar\omega_0)$. Thus, a decoherence rate γ_d can be identified as the term $\kappa^2\gamma_c k_B T/\hbar\omega_0$, which agrees with the earlier-derived estimate (36) up to an overall numerical factor. Approximation (62) clearly shows the washing out of the coherent, oscillatory behavior by the environment when the decoherence time $1/\gamma_d$ is shorter than the cantilever period. When the decoherence time exceeds the dwell time $\hbar/\Gamma$, then the former has a negligible effect on the transmission properties.

C. Results for the cantilever coupled to the environment

The expression for the transmission amplitude including the coupling to the cantilever's environment [Eq. (59)] can be integrated numerically, thereby allowing us to explore the effect on the transmission characteristics of varying the cantilever's Q factor under more general conditions than those for which approximation (62) is justified. Figure 4 shows the magnitude and phase of the transmission amplitude through the dot for $\Gamma/\hbar\omega_0 = 0.5$, $\bar{n} = 18$, and $Q = \omega_0/\gamma_c = 50$. The diagram should be compared with Fig. 3 showing the behavior of the same system without environmental coupling. Figure 5 shows the behavior at resonance of $|\langle t_{\mathrm{QD}}(\epsilon)\rangle|$ for $Q = 50$ and 500, as well as the $\gamma_c/\omega_0 = 0$ (no environment) case for comparison.

It is clear from the figures that the coupling to the environment tends to destroy the side resonances in the transmission amplitude, as well as the associated features in the phase. This is because the environment acts to degrade the coherent superposition of cantilever states into which the interaction with the electron tries to drive the cantilever. Furthermore, the figures show that these environmental effects become increasingly important as the cantilever-electron coupling κ is increased. This is because the larger κ is, the greater is the difference between the states in the superposition into which the cantilever is driven, and consequently the faster is the rate at which the superposition decoheres.

VI. PRACTICAL CONSIDERATIONS

The model parameter ranges actually allowed in an experiment are limited by practical constraints. Up until now we have only referred to these very loosely and have concentrated instead on the range of behavior that can occur in the which-path system under fundamental constraints alone.

Probably the most important practical constraint affects

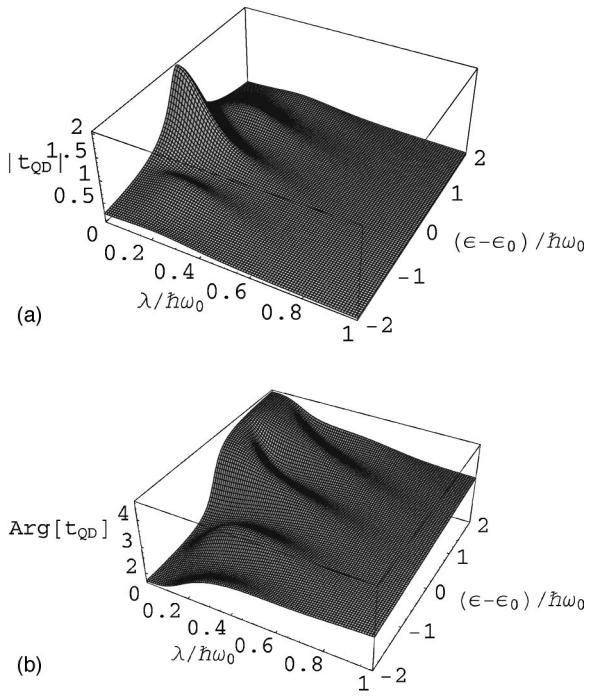

FIG. 4. (a) Magnitude of the transmission amplitude $|\langle t_{\mathrm{QD}}\rangle|$ and (b) the phase for a cantilever with $\Gamma/\hbar\omega_0=0.5$ as a function of the coupling constant, including the effect of the cantilever's environment with $Q=50$ as a function of κ and $\epsilon-\epsilon_0$.

the upper range of the electric field which can be developed between the cantilever and the dot. The maximum allowable field is typically $\sim 10^5$ V/m before a breakdown of the two-dimensional electron gas occurs due to deconfinement,[35] and so we must take this as the largest possible value in considering the practicality of the system.

The temperature of the system is limited by the difficulty of cooling conduction electrons to ultralow temperatures. It becomes extremely difficult to reduce the electron temperature below about 20 mK, because the electrons become practically decoupled from acoustic phonons. Therefore we take 20 mK to be the temperature minimum.

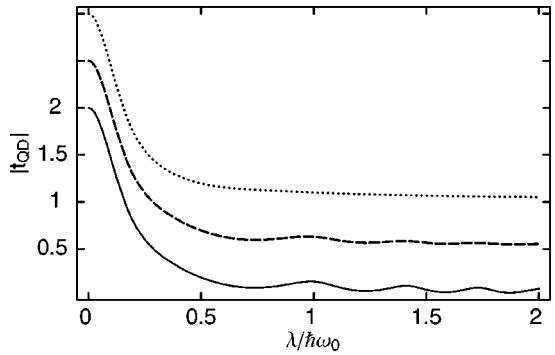

FIG. 5. Magnitude of the resonant transmission amplitude $|\langle t_{\mathrm{QD}}\rangle|$, including the effect of the cantilever's environment as a function of κ for $\Gamma/\hbar\omega_0=0.5$ and $Q=50$ (dotted curve) and 500 (dashed curve). The latter curve has been shifted upwards by 0.5 and the former shifted upwards by 1 for clarity. The case without environmental coupling where $\gamma_c/\omega_0=0$ (full curve) is included for comparison.

The frequency range of the cantilever is crucial for observing quantum coherent behavior such as side resonances, as well as their destruction due to decoherence. The lower limit on the frequency range is set by the requirement that the cantilever period should be comparable to the dwell time $\tau_d=\hbar/\Gamma$ of the electron on the quantum dot, while the upper limit is set by the requirement that the interaction between the cantilever and the electron on the dot be sufficiently strong, given the limits on the electric field, to lead to decoherence, again on a time-scale comparable to the dwell time. The interaction between the electron on the dot and the cantilever is discussed in more detail in Appendix A, along with the geometrical factors that arise in the calculation of the effect of the electric field on the flexural cantilever modes. The dwell time is limited by the rate at which processes other than the interaction with the cantilever cause decoherence, as well as how small a current can be measured through the dot. Of course, the decoherence rate of all the background processes is very difficult to estimate theoretically; in experiment it can be done by observing the visibility of the fringes as a function of dwell time with the cantilever interaction switched off. This then provides a baseline with which to compare all later measurements where we are interested in the effect of the cantilever. Previous experiments carried out at $T=0.1$ K by Yacoby *et al.*,[10] which were designed to measure the phase of the transmission amplitude through a dot in the absence of any external probe, show that dwell times as long 10 ns and currents as low as $\sim 10^{-11}$ A lead to fringes which are still detectable.

It turns out that the best compromise between the two competing frequency limits is achieved by using, say, a carbon nanotube cantilever with a frequency of 100–200 MHz, giving a maximum coupling $\kappa=\lambda/\hbar\omega_0\sim 3$ (Appendix A). The problem is not so much in finding a cantilever with a high enough frequency, but rather in obtaining a large enough coupling from the electric field to cause a detectable amount of dephasing.

In the light of these practical constraints it is clear that only some of the theoretical results obtained in our analysis would be observable in an experiment using current technology. The overall destruction of the AB interference fringes as the coupling between the cantilever and the electron on the dot is increased should be detectable, both in the regime where $\Gamma/\hbar\omega_0\gg 1$ and $\Gamma/\hbar\omega_0\sim 1$. However, the restrictions on the temperature and cantilever frequency imply that an experiment would have to be performed in the regime where $k_{\mathrm{B}}T\gg\hbar\omega_0$. This means that the thermal width of electron energies will wash out the side resonances in the transmission which were found to occur when $\Gamma/\hbar\omega_0\sim 1$. Under these circumstances, the effect of the cantilever's environment on the transmission characteristics would be obscured. However, we emphasize again that these limitations are not fundamental: if the width of the electron energies could be reduced or if the restriction on the maximum cantilever frequency could be relaxed (by finding a way to increase the coupling between the electron on the dot and the cantilever, for example) then the coherent, quantum electromechanical features that our analysis predicts should be observable.

Whilst it is not clear how the coupling constant between the cantilever and the dot could be increased, it is possible to reduce the thermal width of electron energies by using a double quantum dot system rather than a single one as we have considered here.[36]

It is also possible to conduct experiments in which an ac bias is applied to the AB ring. Such an experiment would provide an alternative way of investigating the interaction between the cantilever and its environment: if the ac frequency is higher than the rate γ_c at which the cantilever state changes due to thermal fluctuations then the thermally induced fluctuations in the phase of the interference fringes should be detectable, and distinguishable from the destruction of the interference fringes due to which-path detection. However, a detailed analysis of such an experiment requires extending the theory developed here to include time dependence, and so goes well beyond the present analysis.

VII. CONCLUSIONS AND DISCUSSION

We have carried out a theoretical analysis of a possible solid state which-path interferometer, in which electronic and mechanical degrees of freedom become coupled. The visibility and phase of the interference fringes in the system depend strongly on the coupling between the electron on the dot and the cantilever. The reduction in visibility with increasing coupling is due in part to the cantilever measuring the path taken by the electron and also due to thermal fluctuations in the state of the cantilever.

When the dwell time of the electron on the dot is short compared to the period of the cantilever, the system behaves in a way which is analogous to Einstein's celebrated recoiling slit experiment. In contrast, when the dwell time is comparable to the cantilever's period, the cantilever and the electron on the dot show signs of behaving as a single coherent quantum system, so long as the electrons incident on the dot have a sufficiently narrow energy width. The coherency of the cantilever-dot system is inferred from the appearance of side resonances in the transmission characteristics. Including the cantilever's environment in the analysis, we find that the side resonances are washed out for a small enough oscillator Q factor, while the average decrease in the fringe visibility with increasing coupling to the cantilever is not affected.

The basic feature of the reduction of fringe visibility as a function of the coupling between the electron on the dot and the cantilever should be observable in an experiment using currently available technology. However, the more delicate features, such as the side resonances in the transmission amplitude for long dwell times and the effect of the cantilever's environment on these resonances, will usually be obscured by the energy thermal width of electrons incident on the dot.

There are two important ways in which our analysis could be extended. Most straightforwardly, we could examine what effect using a double dot, rather than a single one, would have on the behavior of the system. In particular, it would be interesting to see to what extent the electron energy width could be reduced, whilst maintaining an overall, measurable current through the device. The second way our analysis could be extended would be to go beyond our steady-state treatment to obtain the time dependence of the transmission amplitude. A time-dependent analysis would allow us to make predictions about the way in which the thermal fluctuations in the state of the cantilever cause fluctuations in the phase of the interference fringes. Such fluctuations may prove to be observable in ac experiments and may also provide us with another way of inferring information about how the cantilever interacts with its environment.

ACKNOWLEDGMENTS

M.P.B. would especially like to thank Eyal Buks for many helpful conversations and invaluable suggestions. Very helpful conversations with Sougato Bose are also gratefully acknowledged. A.D.A. thanks Angus MacKinnon for a series of very useful discussions. Funding was provided by the EPSRC under Grant No. GR/M42909/01.

APPENDIX A: CANTILEVER

The cantilever in the which-path experiment we propose must fulfill a number of quite stringent properties: it must have a fundamental frequency in the range 100–200 MHz and it must also be a conductor. These requirements can be satisfied conveniently by using a carbon nanotube as a cantilever rather than a device which has been fabricated via some kind of etching process from a much larger substrate.

Carbon nanotubes have a number of remarkable physical properties which are beginning to exploited for practical purposes. Recent experiments have seen them employed as hyper-sensitive tips in atomic force microscopy (AFM) experiments, with the nanotube attached to the end of a conventional AFM tip to extend the effective range of resolution of the device.[37] A similar apparatus could be used to bring a nanotube into position to act as the cantilever in our which-path experiment, either in the geometrical configuration explicitly considered above or some variation of it which would lead to slightly different geometrical factors, but not change the underlying linear form of the cantilever-dot interaction.

In this appendix we carry out an analysis of the coupling between the cantilever and the electron on the dot, and the normal modes of a nanotube cantilever. We verify the linear dependence of the cantilever energy on the electric field assumed in the text and derive the form of the coupling constant λ. By examining the mode spectrum of a nanotube cantilever, we confirm the possibility of obtaining a cantilever with a fundamental flexural mode of order 10^8 Hz, and we justify our assumption that for any given cantilever it is sufficient to consider just the lowest mode.

1. Cantilever-dot coupling

We begin by determining the relation between the maximum electric field at the surface of the dot and the voltage applied to the conducting cantilever, before analyzing the details of the effect of the electron on the cantilever energy.

We will consider a cantilever of length $L \sim 1\ \mu$m, positioned so that its tip lies over the center of the dot and at a height $d \sim 0.1\ \mu$m.[24] When an extra electron is added to the

dot it will cause a (classical) vertical displacement of the tip $z \ll d$. We treat the cantilever as a conducting needle, since its length will be far greater than either of the other two dimensions. An applied voltage induces a line charge density σ on the cantilever, but because the cantilever is necessarily finite in length, the charge density is not entirely uniform and so for an exact treatment we should write the line charge density as $\sigma(x)$ where x runs along the length of the cantilever from the tip ($x=0$). However, for a cantilever with a large enough aspect ratio, the charge density can be approximated as constant with only a small error [the error is of order δ with $\delta^{-1}=2\ln(L/r)$, where r is the radius, for a rod-shaped cantilever[38]]. For the cantilever we are considering the radius may be as small as 1.5 nm, as we discuss below, and so the error in assuming a uniform charge density will be less than 10%, which is acceptable as our aim is to obtain an order of magnitude estimate for the interaction strength.

The charge induced on the cantilever leads to an electric field at the surface of the dot,

$$\mathbf{E}=\int_0^L \frac{\sigma(-x\hat{\mathbf{i}}+d\hat{\mathbf{j}})dx}{4\pi\epsilon_0(x^2+d^2)^{3/2}}, \tag{A1}$$

taking $\sigma=cV$ where c is an unimportant constant and V is the voltage applied to the cantilever. The unit vectors are defined so that $\hat{\mathbf{i}}$ runs along the cantilever away from its tip and $\hat{\mathbf{j}}$ points down from the tip towards the dot. Since $L \gg d$, we find

$$|\mathbf{E}| \simeq \frac{2^{1/2}cV}{4\pi\epsilon_0 d}. \tag{A2}$$

We also need to know how the potential energy of the cantilever varies for small vertical displacements z about the equilibrium position d_0, where $d=d_0-z$. For a section of the cantilever of length Δx centered at x, the potential energy due to the displacement is

$$\Phi(x)=\frac{qcV\Delta x}{4\pi\epsilon_0\sqrt{(d_0-z)^2+x^2}}, \tag{A3}$$

where $q=-e$ is the excess charge on the dot. Since $d_0 \gg z$, we obtain the z-dependent part of the potential energy as

$$\Phi_z(x)=z\frac{qcVd_0\Delta x}{4\pi\epsilon_0(d_0^2+x^2)^{3/2}}. \tag{A4}$$

This is of course linear in z as we anticipated in our model. However, in order to obtain the effective coupling between the electric field and each of the cantilever modes we need to rewrite the z-dependent part of the potential energy in terms of the normal modes of the cantilever and so we turn now to the mode spectrum of the cantilever.

2. Cantilever modes

A single-walled nanotube cantilever can be obtained with lengths ~ 1 μm, diameters ~ 3 nm, and a Young's modulus ~ 1 TPa.[39] Recent experiments[29,40] have shown that the flexural modes of such nanotubes have frequencies which lie in the MHz-GHz regime. We can treat a nanotube as a rigid hollow rod and so obtain the frequencies of the flexural modes,[41]

$$\omega_i=\frac{\beta_i^2}{2L^2}\sqrt{\frac{Y(a^2+b^2)}{\rho}}, \tag{A5}$$

where a and b are the outer and inner diameters, L the length, Y the Young's modulus, and ρ the density of the tube. The factors β_i arise from geometrical considerations and are the solutions of the equation $\cos(\beta_i)\cosh(\beta_i)=-1$.

The energy of the cantilever can be written in terms of its classical normal modes as

$$H=\sum_i \left(\frac{1}{2}m\omega_i^2 q_i^2+\frac{p_i^2}{2m}\right)I_i, \tag{A6}$$

where

$$I_i=\frac{1}{L}\int_0^L \Gamma_i^2 dx \tag{A7}$$

and

$$\begin{aligned}\Gamma_i(L-x)=&[\cos(\beta_i)+\cosh(\beta_i)][\sin(\beta_i x/L)-\sinh(\beta_i x/L)]\\&-[\sin(\beta_i)+\sinh(\beta_i)][\cos(\beta_i x/L)\\&-\cosh(\beta_i x/L)]\end{aligned} \tag{A8}$$

are the vibrational mode eigenfunctions.[41] If we modify the definitions of the canonical variables slightly to define $q_i'=q_i I_i^{1/2}$ and $p_i'=p_i I_i^{1/2}$, then the Hamiltonian takes the conventional form

$$H=\sum_i \left(\frac{1}{2}m\omega_i^2 (q_i')^2+\frac{(p_i')^2}{2m}\right). \tag{A9}$$

We can add in the additional potential energy due to small amplitude deflections in the electric field by expanding the displacement z in terms of the normal modes,

$$V(z)=-\sum_i \frac{ecVd_0}{4\pi\epsilon_0 I_i^{1/2}}\left(\int_0^L \frac{\Gamma_i(x)dx}{[(x-L)^2+d_0^2]^{3/2}}\right)q_i', \tag{A10}$$

where the origin of x has been shifted.

We can quantize the full Hamiltonian for the cantilever in the usual way, and so we are able to associate a position operator of the form

$$\hat{q}_i'=\left(\frac{\hbar}{2m\omega_i}\right)^{1/2}(\hat{a}_i^\dagger+\hat{a}_i) \tag{A11}$$

with each mode. Thus, it follows that the interaction between the electron on the dot and the cantilever can be written in the form proposed [Eq. (11)] with a coupling constant between the cantilever and the dot which depends on the mode we are considering

$$\lambda_i=eE\xi_i\sqrt{\frac{\hbar}{2m\omega_i}}, \tag{A12}$$

where ξ_i is a dimensionless constant of order unity defined by the relation

$$\xi_i = \frac{d_0^2}{(2I_i)^{1/2}} \int_0^L \frac{\Gamma_i(x)dx}{[(x-L)^2+d_0^2]^{3/2}}. \tag{A13}$$

We can see from Eqs. (19) and (24) that the effect of a particular cantilever mode on the electron interference in the which-path device depends on $(\lambda_i/\hbar\omega_i)^2$ rather than on λ_i alone. Thus, the ratio of the coupling between the fundamental and the ith excited mode goes as $(\omega_0/\omega_i)^3=(\beta_0/\beta_i)^6$. Because the electric field is strongly limited, we will always be working in the regime where the coupling constant is just sufficient to cause detectable effects. Therefore, since $(\beta_0/\beta_1)^6 \sim 0.005$, our assumption that only the fundamental mode is relevant is justified.

As a concrete example, we consider a nanotube cantilever of length 1.4 μm and outer radius 3.3 nm.[39] In this case, the fundamental frequency is 140 MHz and the mass is of order 8×10^{-20} kg. If the tip-dot distance is set at ~ 0.1 μm, then $\xi_0 \sim 1.3$ and for a maximum electric field of 10^5 V/m, the corresponding maximum coupling constant $\kappa=\lambda/\hbar\omega_0 \sim 3$.

APPENDIX B: NONPERTURBATIVE CALCULATION OF ENVIRONMENTAL COUPLING

In Sec. V we calculated the transmission amplitude through the dot, including the effect of the cantilever's environment, by expanding to second order in the interaction between the cantilever and the electron on the dot λ, and then reexponentiating. In this appendix we justify this result with a full calculation. The fact that a second-order expansion in λ leads to the exact result is at first somewhat surprising. However, the important step is the reexponentiation of the truncated series expansion (52): we implicitly equate the influence functional with not just the first few terms in an expansion, but with an infinite series of terms which are themselves composed of products of the second-order terms we evaluated. This procedure is generally acceptable as an approximation in the limit of small λ, but in this particular case the series generated in fact coincides with the exact form obtained from a linked cluster expansion.[42]

We begin by adopting the notation

$$\hat{O}(t) = -e^{(-i\omega_0-\gamma)t}\int_0^t dt'\hat{F}(t')e^{(i\omega_0+\gamma)t'},$$

$$\hat{O}^\dagger(t) = -e^{(i\omega_0-\gamma)t}\int_0^t dt'\hat{F}^\dagger(t')e^{(-i\omega_0+\gamma)t'},$$

so that

$$\hat{a}(t) = \hat{a}(0)e^{(-i\omega_0-\gamma)t} + \hat{O}(t),$$

$$\hat{a}^\dagger(t) = \hat{a}^\dagger(0)e^{(+i\omega_0-\gamma)t} + \hat{O}^\dagger(t).$$

The operators $\hat{O}(t)$ and $\hat{O}^\dagger(t)$ operate only on the variables of the oscillator bath and they both commute with $\hat{a}(0)$ and $\hat{a}^\dagger(0)$ which operate on the states of the cantilever alone.

The object that we wish to evaluate is the influence functional

$$\begin{aligned}\langle \mathrm{T}_t e^{-i\int_0^t W_I(t')dt'/\hbar}\rangle &= \langle \mathrm{T}_t e^{i\lambda\int_0^t[\hat{a}(0)e^{(-i\omega_0-\gamma)t'}+\hat{a}^\dagger(0)e^{(+i\omega_0-\gamma)t'}]dt'/\hbar}\rangle \\ &\times \langle \mathrm{T}_t e^{i\lambda\int_0^t[\hat{O}(t')+\hat{O}^\dagger(t')]dt'/\hbar}\rangle,\end{aligned} \tag{B1}$$

where we have exploited the commutation properties of the operators to factor the expression into two terms, which we can now write as $C_1\times C_2$.

The method we use to evaluate C_1 and C_2 is based on the application of Wick's theorem, as described in the books by Mahan[42] and Louisell.[34] We can write the first term as

$$\begin{aligned}C_1 &= \langle \mathrm{T}_t e^{i\lambda[\int_0^t \hat{a}(0)e^{(-i\omega_0-\gamma)t'}+\hat{a}^\dagger(0)e^{(+i\omega_0-\gamma)t'}]dt'/\hbar}\rangle \\ &= \sum_{n=0}^{\infty} i^n U_n(t),\end{aligned} \tag{B2}$$

where

$$\begin{aligned}U_n(t) = \frac{(\lambda/\hbar)^n}{n!}\int_0^t dt_1\cdots\int_0^t dt_n \langle \mathrm{T}_t[\hat{a}(0)e^{(-i\omega_0-\gamma)t_1} \\ +\hat{a}^\dagger(0)e^{(+i\omega_0-\gamma)t_1}]\cdots[\hat{a}(0)e^{(-i\omega_0-\gamma)t_n} \\ +\hat{a}^\dagger(0)e^{(+i\omega_0-\gamma)t_n}]\rangle.\end{aligned}$$

An obvious simplification arises from the fact that the averages over odd numbers of operators will always vanish and so we can replace n by the even index $2m$.

We now apply Wick's theorem which allows us to write the average of products of pairs of operators as products of the averages of pairs of operators. Thus for U_{2m}, we have

$$\begin{aligned}U_{2m} = \frac{(\lambda/\hbar)^{2m}i^{2m}}{(2m)!}\int_0^t dt_1\cdots\int_0^t dt_{2m} \\ \times\sum_C \{D_0(t_1-t_i)\cdots D_0(t_j-t_{2m})\},\end{aligned} \tag{B3}$$

where the summation is over all possible pairing combinations of the $2m$ time labels and

$$\begin{aligned}iD_0(t_1-t_2) = \langle \mathrm{T}_t[\hat{a}(0)e^{(-i\omega_0-\gamma)t_1}+\hat{a}^\dagger(0)e^{(+i\omega_0-\gamma)t_1}] \\ \times[\hat{a}(0)e^{(-i\omega_0-\gamma)t_2}+\hat{a}^\dagger(0)e^{(+i\omega_0-\gamma)t_2}]\rangle.\end{aligned} \tag{B4}$$

The summation over all possible combinations for each term allows us to reexponentiate so that $C_1 = e^{-\phi_0(t)}$, where

$$\phi_0(t) = \frac{i}{2}\left(\frac{\lambda}{\hbar}\right)^2\int_0^t dt_1\int_0^t dt_2 D_0(t_1-t_2). \tag{B5}$$

It is important to notice that the exact form of the function of time and frequency multiplying the operators $\hat{a}(0)$ and $\hat{a}^\dagger(0)$ is unimportant. These functions give the operators their individual time labels, but because they are just algebraic functions they do not affect the validity of Wick's theorem.

Now we must consider the second term,

$$C_2=\langle e^{i\lambda\int_0^t[\hat{O}(t)+\hat{O}^\dagger(t)]dt'/\hbar}\rangle. \tag{B6}$$

We can make progress by separating out the underlying operators of the oscillators in the bath

$$\hat{O}(t)=-e^{(-i\omega_0-\gamma)t}\int_0^t dt'\sum_\omega \hat{A}(\omega,0)g(\omega)e^{-i\omega t'}e^{(i\omega_0+\gamma)t} \tag{B7}$$

$$=\sum_\omega \hat{A}(\omega,0)g(\omega) \times\left[-e^{(-i\omega_0-\gamma)t}\int_0^t dt' e^{-i\omega t'}e^{(i\omega_0+\gamma)t'}\right] \tag{B8}$$

$$=\sum_\omega \hat{A}(\omega,0)g(\omega)f(\omega,\omega_0,\gamma,t) \tag{B9}$$

and similarly,

$$\hat{O}^\dagger(t)=\sum_\omega \hat{A}^\dagger(\omega,0)g^*(\omega)f^*(\omega,\omega_0,\gamma,t). \tag{B10}$$

We do not need to calculate f explicitly since it is just an algebraic function and so always commutes. Because the oscillators in the heat bath are all noninteracting, almost all the $\hat{A}(\omega,0)$ and $\hat{A}^\dagger(\omega,0)$ operators commute. The only exceptions are annihilation and creation operators of the same frequency. This means that we can write the expectation value as a product over all the frequencies,

$$C_2=\prod_\omega \langle e^{i\lambda\int_0^t[\hat{A}(\omega,0)g(\omega)f+\hat{A}^\dagger(\omega,0)g^*(\omega)f^*]dt'/\hbar}\rangle. \tag{B11}$$

The advantage of decoupling C_2 into a product of terms is that each of these terms can be handled in the same way as C_1. Because $\hat{A}(\omega,0)$ and $\hat{A}^\dagger(\omega,0)$ are boson operators, Wick's theorem can again be applied so that eventually we obtain

$$C_2=\prod_\omega e^{-\phi_\omega(t)}, \tag{B12}$$

where

$$\phi_\omega(t)=\frac{i\lambda^2}{2\hbar^2}\int_0^t dt_1\int_0^t dt_2 D_\omega(t_1-t_2), \tag{B13}$$

with

$$iD_\omega(t_1-t_2)=\langle \mathrm{T}_t[\hat{A}(\omega,0)g(\omega)f(\omega,\omega_0,\gamma,t_1) +\hat{A}^\dagger(\omega,0)g^*(\omega)f^*(\omega,\omega_0,\gamma,t_1)] \times[\hat{A}(\omega,0)g(\omega)f(\omega,\omega_0,\gamma,t_2) +\hat{A}^\dagger(\omega,0)g^*(\omega)f^*(\omega,\omega_0,\gamma,t_2)]\rangle. \tag{B14}$$

The overall expression for the influence functional can now be written in a simplified form

$$\langle \mathrm{T}_t e^{-i\int_0^t W_I(t')dt'/\hbar}\rangle=e^{-[\phi_0(t)+\Sigma_\omega\phi_\omega(t)]}=e^{-\phi(t)}, \tag{B15}$$

where

$$\phi(t)=\frac{i\lambda^2}{\hbar^2}\int_0^t dt_1\int_0^{t_1} dt_2\left\{D_0(t_1-t_2)+\sum_\omega D_\omega(t_1-t_2)\right\}. \tag{B16}$$

However, because the operators in the bath are independent, only the averages including pairs of operators from the same oscillator are nonzero. Thus, we can simplify the sum over $D_\omega(t)$ functions,

$$\sum_\omega D_\omega(t_1-t_2)=\sum_\omega \langle[\hat{A}(\omega,0)g(\omega)f(\omega,\omega_0,\gamma,t_1) +\hat{A}^\dagger(\omega,0)g^*(\omega)f^*(\omega,\omega_0,\gamma,t_1)] \times[\hat{A}(\omega,0)g(\omega)f(\omega,\omega_0,\gamma,t_2) +\hat{A}^\dagger(\omega,0)g^*(\omega)f^*(\omega,\omega_0,\gamma,t_2)]\rangle \tag{B17}$$

$$=\langle[\hat{O}(t_1)+\hat{O}^\dagger(t_1)][\hat{O}(t_2)+\hat{O}^\dagger(t_2)]\rangle. \tag{B18}$$

Since the $\hat{O}(t)$ and $\hat{O}^\dagger(t)$ operators commute with $\hat{a}(0)$ and $\hat{a}^\dagger(0)$ we can complete the process of recombination to obtain

$$i\left\{D_0(t_1-t_2)+\sum_\omega D_\omega(t_1-t_2)\right\} =\langle[\hat{a}(t_1)+\hat{a}^\dagger(t_1)][\hat{a}(t_2)+\hat{a}^\dagger(t_2)]\rangle. \tag{B19}$$

We can now use our previous results in Eqs. (55), (57), and (58) to evaluate the averages in Eq. (B19),

$$\langle[\hat{a}(t_1)+\hat{a}^\dagger(t_1)][\hat{a}(t_2)+\hat{a}^\dagger(t_2)]\rangle =e^{-\gamma(t_1-t_2)}[(\bar{n}+1)e^{-i\omega_0(t_1-t_2)}+\bar{n}e^{i\omega_0(t_1-t_2)}]. \tag{B20}$$

Thus, our final expression for the influence functional is

$$\langle \mathrm{T}_t e^{-i\int_0^t W_I(t')dt'/\hbar}\rangle=e^{-\phi(t)}, \tag{B21}$$

with

$$\phi(t)=\frac{\lambda^2}{\hbar^2}\int_0^t dt_1\int_0^{t_1} dt_2 e^{-\gamma(t_1-t_2)}[(\bar{n}+1)e^{-i\omega_0(t_1-t_2)} +\bar{n}e^{i\omega_0(t_1-t_2)}]. \tag{B22}$$

Comparing Eq. (B22) with Eq. (60) it is clear that the expression we obtained for the influence functional in Sec. V is exact.

*Electronic address: a.armour@ic.ac.uk
†Electronic address: miles.p.blencowe@dartmouth.edu

[1] N. Bohr, in *Albert Einstein: Philosopher Scientist*, edited by P. A. Schilpp (Library of Living Philosophers, Evanston, IL, 1949), Vol. 7, p. 200.
[2] R. Feynman, R. Leighton, and M. Sands, *The Feynman Lectures on Physics* (Addison-Wesley, MA, 1965), Vol. III.
[3] E. Buks, R. Schuster, M. Heiblum, D. Mahalu, and V. Umansky, Nature (London) **391**, 871 (1998).
[4] S. Dürr, T. Nonn, and G. Rempe, Nature (London) **395**, 33 (1998).
[5] W. K. Wooters and W. H. Zurek, Phys. Rev. D **19**, 473 (1979).
[6] M. O. Scully, B.-G. Englert, and H. Walther, Nature (London) **351**, 111 (1991).
[7] P. Storey, S. Tan, M. Collett, and D. Walls, Nature (London) **367**, 626 (1994).
[8] A. Stern, Y. Aharonov, and Y. Imry, Phys. Rev. A **41**, 3436 (1990).
[9] For a review of previous work on phase coherent transport and controlled dephasing see G. Hackenbroich, /cond-mat/0006361 (unpublished).
[10] A. Yacoby, M. Heiblum, D. Mahalu, and H. Shtrikman, Phys. Rev. Lett. **74**, 4047 (1995).
[11] G. Hackenbroich, B. Rosenow, and H. A. Weidenmüller, Europhys. Lett. **44**, 693 (1998).
[12] Y. Levinson, Europhys. Lett. **39**, 299 (1997).
[13] I. L. Aleiner, N. S. Wingreen, and Y. Meir, Phys. Rev. Lett. **79**, 3740 (1997).
[14] S. A. Gurvitz, Phys. Rev. B **56**, 15 215 (1997).
[15] S. Mancini, V. I. Man'ko, and P. Tombesi, Phys. Rev. A **55**, 3042 (1997); S. Bose, K. Jacobs, and P. L. Knight, *ibid.* **56**, 4175 (1997).
[16] S. Bose, K. Jacobs, and P. L. Knight, Phys. Rev. A **59**, 3204 (1999).
[17] S. Datta, *Electronic Transport in Mesoscopic Structures* (Cambridge University Press, Cambridge, U.K., 1995).
[18] M. Büttiker, IBM J. Res. Dev. **32**, 317 (1988).
[19] A. Levy Yeyati and M. Büttiker, Phys. Rev. B **52**, R14 360 (1995).
[20] Y. Imry, *Introduction to Mesoscopic Physics* (Oxford University Press, Oxford, U.K., 1997).
[21] A. Yacoby, R. Schuster, and M. Heiblum, Phys. Rev. B **53**, 9583 (1996).
[22] Our assumption is that the which-path device is operated in a steady-state mode, whereby measurements are only made after any transitory behavior has decayed so that the probability distribution of (initial) cantilever states is stationary. This steady-state distribution is further assumed to be the usual thermal distribution. These assumptions will only be strictly correct in the limit as the current goes to zero, but can be expected to provide predictions which are at least qualitatively correct for the average behavior over long times even with finite currents.
[23] P. D. D. Schwindt, P. G. Kwiat, and B.-G. Englert, Phys. Rev. A **60**, 4285 (1999).
[24] We assume that all positions are measured from the equilibrium height of the cantilever above the dot, including the effect of the residual electrons on the dot which do not participate in the transport.
[25] N. S. Wingreen, K. W. Jacobsen, and J. W. Wilkins, Phys. Rev. B **40**, 11 834 (1989).
[26] L. I. Glazman and R. I. Shekhter, Zh. Éksp. Teor. Fiz. **94**, 292 (1987) [Sov. Phys. JETP **67**, 163 (1988)].
[27] A.-P. Jauho and N. S. Wingreen, Phys. Rev. B **58**, 9619 (1998).
[28] W. G. Unruh and W. H. Zurek, Phys. Rev. D **40**, 1071 (1989).
[29] P. Poncharal, Z. L. Wang, D. Ugarte, and W. A. de Heer, Science **283**, 1513 (1999).
[30] A. O. Caldeira and A. J. Leggett, Ann. Phys. (N.Y.) **149**, 374 (1983).
[31] R. Omnès, *The Interpretation of Quantum Mechanics* (Princeton University Press, Princeton, NJ, 1994).
[32] E. Joos and H. D. Zeh, Z. Phys. B: Condens. Matter **59**, 223 (1985).
[33] L. Mandel and E. Wolf, *Optical Coherence and Quantum Optics* (Cambridge University Press, Cambridge, U.K., 1995).
[34] W. Louisell, *Quantum Statistical Properties of Radiation* (Wiley, New York, 1973).
[35] E. Buks (private communication).
[36] D. Sprinzak, E. Buks, M. Heiblum, and H. Shtrikman, Phys. Rev. Lett. **84**, 5820 (2000).
[37] R. M. D. Stevens, N. A. Frederick, B. L. Smith, D. E. Morse, G. D. Stucky, and P. K. Hansma, Nanotechnology **11**, 1 (2000).
[38] J. D. Jackson, Am. J. Phys. **68**, 789 (2000).
[39] M. M. J. Treacy, T. W. Ebbesen, and J. M. Gibson, Nature (London) **381**, 678 (1996).
[40] B. Reulet, A. Y. Kasumov, M. Kociak, R. Deblock, I. I. Khodos, Y. B. Gorbatov, V. T. Volkov, C. Journet, and H. Bouchiat, Phys. Rev. Lett. **85**, 2829 (2000).
[41] H.-J. Butt and M. Jashchke, Nanotechnology **6**, 1 (1995).
[42] G. Mahan, *Many-Particle Physics*, 2nd ed. (Plenum Press, New York, 1990).